Dimethyloxalyl Glycine Regulates the HIF-1 Signaling Pathway in Mesenchymal Stem Cells

Binjie Zhou[1] · Tingting Ge[1] · Liping Zhou[1] · Lixia Jiang[1] · Lujie Zhu[1] · Panpan Yao[1] · Qin Yu[1]

Abstract

Mesenchymal stem cells (MSCs) are pluripotent stem cells with self-renewal and multidirectional differentiation capabilities. Dimethyloxalyl glycine (DMOG) mobilizes MSCs, and the hypoxia inducible factor-1 (HIF-1) signaling pathway plays an important role in MSC mobilization. We aimed to investigate the effect of DMOG on the HIF-1 pathway in MSCs. Rats were treated with DMOG, and the numbers of peripheral blood MSCs (PB-MSCs) and bone marrow MSCs (BM-MSCs) were detected by the Colony-forming unit fibroblastic (CFU-F) method. The growth curve, cell cycle and migration ability of PB-MSCs and BM-MSCs were detected by CCK-8, Flow cytometry and Transwell assays. Western blotting and real-time qPCR were used to detect the expression of the HIF-1 pathway. The number of bone marrow microvessels was detected by immunohistochemistry. DMOG significantly increased the numbers of PB-MSCs and BM-MSCs ($P < 0.05$). Further, the MSCs in peripheral blood and bone marrow still had the ability to proliferate and migrate after mobilization by DMOG. The expression levels of HIF-1α, stromal cell-derived factor-1α (SDF-1α) and vascular endothelial growth factor (VEGF) in MSCs were significantly regulated by DMOG ($P < 0.05$). The number of bone marrow microvessels decreased after the VEGF/VEGFR signaling pathway was blocked by SU5416 ($P < 0.05$). Therefore, these findings demonstrated that DMOG regulates the HIF-1α signaling pathway and promotes biological effects in MSCs.

Keywords Dimethyloxalyl glycine · Hypoxia inducible factor-1α · Mesenchymal stem cell · Stromal cell-derived factor-1α · Vascular endothelial growth factor

Binjie Zhou and Tingting Ge contributed equally to this work.

✉ Qin Yu
19891006@zcmu.edu.cn

Binjie Zhou
201811114211525@zcmu.edu.cn

Tingting Ge
201612200502016@zcmu.edu.cn

Liping Zhou
20141026@zcmu.edu.cn

Lixia Jiang
201612200503015@zcmu.edu.cn

Lujie Zhu
201711115311545@zcmu.edu.cn

Panpan Yao
201512202302037@zcmu.edu.cn

[1] College of Life Science, Zhejiang Chinese Medical University, 548 Binwen Road, Hangzhou, Zhejiang 310053, People's Republic of China

Introduction

Mesenchymal stem cells (MSCs) are a type of adult stem cells with extensive sources, strong proliferative capacity and multidirectional differentiation potential. Currently, transplantation is the main clinical application of MSCs [1, 2]. However, a series of disadvantages restrict its clinical application, such as limited cell sources for transplantation, pollution problems and tumorigenic risk. Mobilization of MSCs, which can avoid these disadvantages [3–7], includes the use of a mobilization agent or mobilization measures to promote the release and migration of MSCs from bone marrow to peripheral blood [8].

Many cytokines and drugs stimulate a series of cell signaling transduction events and also mobilize numerous stem/progenitor cells from the bone marrow microenvironment, thus inducing migration of these cells into peripheral blood [9–11]. Hypoxia inducible factor-1α (HIF-1α) has been reported as a key factor of MSC mobilization [12, 13]. HIF-1 is the core transcription factor of the hypoxia response in the organism, and its α-subunit is a functional subunit regulated

by hypoxia. In normal oxygen conditions, HIF-1α is rapidly degraded by hydroxylation of prolylhydroxylase (PHD), which is also the rate-limiting enzyme of HIF degradation. Proline hydroxylase inhibitors (PHIs) inhibit the activity of PHD and reduce the degradation of HIF-1α under constant oxygen conditions. PHI stabilizes HIF-1α levels and upregulates the HIF-1 signaling pathway by inhibiting the hydroxylation of HIF-1α. Dimethyloxalyl glycine (DMOG) is a type of PHI that inhibits PHD by competing with endogenous 2-ketoglutarate [14–16].

We have previously reported that DMOG mobilizes MSCs [11]. Stromal cell-derived factor-1α (SDF-1α) and its receptor, C-X-C motif chemokine receptor (CXCR4), are associated with stem cell migration and injury repair [17–19]. SDF-1α and CXCR4 are enhanced after promoting HIF-1α by signaling molecules [20]. Vascular endothelial growth factor (VEGF) plays a central role on angiogenesis [21], which promotes endothelial cell proliferation and neovascularization, and enhances vascular permeability by promoting tyrosine protein kinase activity in combination with its specific receptor, VEGFR [22]. The VEGF/VEGFR signaling pathway is a pathway that mediates changes in the bone marrow microenvironment and the migration of MSCs [23].

In the present study, we investigated the effects of DMOG on the number, growth curve, cell cycle, and migration of MSCs in rats. The expression levels of HIF-1α, SDF-1α and VEGF were analyzed, and the number of bone marrow microvessels in rats was also analyzed.

Materials and Methods

Animals Male Sprague-Dawley rats (80–100 g) were provided by the Zhejiang Chinese Medical University Animal Center (Laboratory Animal Certificate: SYXK 2013–0184). All procedures related to the use of animals complied with the guide published by NIH.

Animal Grouping Rats were divided into a normal saline (NS) group (treated with normal saline) and DMOG group (40 mg/kg DMOG). To explore the effect of DMOG on mobilizing MSCs, the number of MSCs in peripheral blood and bone marrow were detected by colony-forming unit fibroblastic (CFU-F). The growth curve, cell cycle, and migration ability of MSCs in peripheral blood and bone marrow were detected by CCK-8, Flow cytometry and Transwell assays. The number of bone marrow microvessels is one of the factors that affects stem cell mobilization [24]. To investigate the effect of DMOG on microvessels, rats were divided into five groups (four rats in each) as follows: NS group (treated with normal saline), DMOG group (40 mg/kg DMOG), YC-1 group (10 mg/kg YC-1 and 40 mg/kg DMOG), AMD3100 group (5 mg/kg AMD3100 and 40 mg/kg DMOG), and SU5416

treatment group (5 mg/kg SU5416 and 40 mg/kg DMOG). YC-1 is HIF-1α-targeted inhibitor, AMD3100 blocks SDF-1α receptor CXCR4, and SU5416 is an inhibitor of VEGF receptor tyrosine kinase [25–28]. All rats were administered by intraperitoneal injection for 7 days. The number of bone marrow microvessels was detected by immunohistochemistry.

Bone Marrow and Peripheral Blood Cell Preparation Rats were anesthetized with 10% chloral hydrate (3.5 mL/kg, Sigma). Peripheral blood (5 mL) was collected from the abdominal aorta. Peripheral blood mononuclear cells were isolated with lymphocyte separation (Hao Yang Biological Manufacture Co., Tianjin, China) medium by the density gradient centrifugation method. Bone marrow was obtained from rat femoral and tibialis tissues. Muscle, connective tissue, fat and epiphyses were removed. The contents of the bone marrow were flushed into a culture dish by using phosphate buffer saline (PBS) (Dingguo Changsheng Biotechnology, China) and treated with 1:2 erythrocyte lysate (BOSTER, China) for 5 min.

Colony-Forming Unit Fibroblastic Assay For CFU-F assays, MSCs derived from peripheral blood and bone marrow cells in each group were placed in a 25 cm$_2$ culture flask with proliferation culture medium, consisting of DMEM/F12 supplemented with 20% (vol/vol) fetal bovine serum (FBS) (Gibco), at a density of 3×10^6 cells/mL. Peripheral blood CFU-Fs and bone marrow CFU-Fs were counted on day 14. A colony (>50 cells) was marked as one CFU-F.

Generation and Culture of MSCs A previously reported method was used for the generation and culture of MSCs [13]. Bone marrow MSCs (BM-MSCs) and peripheral blood MSCs (PB-MSCs) were purified over multiple generations.

Growth Curve of MSCs Following cell counting, PB-MSCs and BM-MSCs (P4) were resuspended in Dulbecco's modified Eagle medium-nutrient mixture F-12 (DMEM/F12) (Gibco) supplemented with 20% (vol/vol) FBS at a density of 3×10^4 cells/mL. The cell suspension was cultured in 96 well plates (200 μL per well) for 24 h, and blank medium was set as the control group. CCK-8 reagent (20 μL, Dojindo) was added to each well, and the plate was incubated at 37 °C for 2 h. The absorbance value at 450 nm was measured by an enzyme labeling instrument and was repeated at the same time for 7 days.

Cell Cycle of MSCs PB-MSCs and BM-MSCs were grown to the fourth generation, and 1×10^6 cells were removed and fixed with 75% precooled ethanol overnight at 4 °C. The next day, cells were mixed with 100 μL RNaseA reagent for 10 min and incubated with PI solution for 30 min.

Migration Ability of MSCs After digestion and counting, fourth generation PB-MSCs and BM-MSCs were resuspended in DMEM/F12 containing 20% FBS and 1% streptomycin, and 150 μL of cell suspension was inoculated into the upper chamber of a Transwell. DMEM/F12 medium (600 μL) containing 200 ng/mL SDF-1α, 20% FBS, and 1% green streptomycin was added to the subchamber. The transwell chamber (Greiner) was placed in a 37 °C incubator for 16 h. The next day, the chamber was removed, and the culture medium was discarded. After removing unmigrated MSCs from the upper layer of the chamber, it was stained with crystal violet and photographed under an inverted phase contrast fluorescence microscope.

Immunohistochemical Analysis Femur and tibia were harvested from rats in each group and fixed in 4% paraformaldehyde for 24 h. Dissected femurs were decalcified in EDTA decalcification solution for 2 weeks at 4 °C. Bone marrow tissue was immersed in xylene, absolute ethanol, 95% ethanol and 75% ethanol for 20 min, 5 min, 5 min, 5 min in sequence. Following paraffin embedding and sectioning, bone marrow tissue sections were heated for 10 min in 0.01 M sodium citrate buffer (95 °C and pH 6.0). Sections were incubated overnight at 4 °C with anti-VEGF antigen mAb (1:5) (Abcam, USA). Envision working solution was added, and sections were incubated at room temperature for 30 min. After washing, visualizing, and restaining, sections were quantified manually in 5 randomly selected high-power microscope fields for each region (200×) by using the following equation: proportion of positive index = number of positive cells in visual field/number of total cells in visual field * 100%.

Cell Grouping To investigate the mechanism of MSC mobilization from bone marrow into peripheral blood by DMOG in vitro, BM-MSCs were divided into the following four groups namely: control group, DMOG group, control siRNA group, and HIF-1α siRNA group. HIF-1α was blocked by treating BM-MSCs with HIF-1α siRNA, and the expression levels of HIF-1α, SDF-1α and VEGF were detected by Western blotting and real-time qPCR.

SiRNA Assay The HIF-1α siRNA sequence was designed and constructed by Invitrogen. MSCs were transfected by the positive control siRNA named Block-IT™ Alexa Fluor® Red Fluorescent oligo (Invitrogen, Grand Island, NY, USA) using Lipofectamine® RNAiMAX. According to the transfection method for the siRNA positive control, the control siRNA concentrations were 10, 30 and 50 pM. After transfection, MSCs were incubated at 37 °C with 5% CO₂. After treatment for 24 h, medium was discarded. The positive cell rate was measured by using an inverted phase contrast fluorescence microscope (Nikon), and the ratio of red fluorescent cells

was the transfection efficiency. The optimal siRNA concentration was used in subsequent transfection experiments.

Western Blotting Total cellular protein was extracted, and the protein concentration was then detected by the BCA method. After SDS-PAGE, protein was transferred to semidry membranes and then incubated with primary antibodies (rabbit antibody against rat β-actin, rabbit antibody against rat HIF-1α, rabbit antibody against rat SDF-1α and rabbit antibody against rat VEGF; Abcam, USA) followed by incubation with secondary antibody (goat anti-rabbit secondary antibody; Abcam, USA). Membranes were then imaged by using the chemiluminescence imaging system, and quantitative analysis was performed with Image J analysis software (National Institutes of Health, USA). The grayscale image of the target band was compared to that of the β-actin band, and the relative expression of the target protein was represented by the ratio.

Real-Time qPCR Primers for HIF-1α, SDF-1α and VEGF were verified against sequences from National Center for Biotechnology Information (NCBI) GenBank and designed according to the principles of SYBR Green I Real-time qPCR. Primers were synthesized by Biological Engineering Co., Ltd. (Shanghai, China). qPCR was performed using the following primers (5′-3′): HIF-1α Fwd: ATCAAGTCAGCAAC GTGGAAG, Rev.: CGTCATAGGCGGTTTCTTGTA; SDF-1α Fwd: CTGAGGCAGGAGTGTGAGGT, Rev.: ACGGTGATGGATGAGACAGA; and VEGF: Fwd: CTGCTGTGGACTTGAGTTGG Rev.: CAAACAGA CTTCGGCCTCTC. qPCR was performed according to the instructions of the PrimeScript™ RT Master Mix kit (Takara), and the synthesized cDNA was used to amplify the target gene according to the instructions of the SYBR® Premix Ex Taq™ II (TliRnaseH Plus) kit. StepOne Software v2.2.2 was used to calculate the sample target gene results. The change of fluorescence intensity reflected the change of template product in a certain concentration range, and real-time quantitative analysis was achieved by analyzing fluorescence intensity. Melting curves were used to analyze each product, and quantitative analysis was performed using the $2^{-\triangle\triangle Ct}$ method.

Statistical Analysis All data were expressed as the mean ± standard deviation (SD). Statistical differences between groups were analyzed with one-way analysis of variance (ANOVA). Comparisons between two groups were performed via Dunnett's t test. $P < 0.05$ was considered statistically significant.

Results

MSCs are Mobilized into Peripheral Blood by DMOG The number of MSCs in peripheral blood and bone marrow was

measured by the CFU-F method to determine if MSCs were mobilized by DMOG. Compared to the NS group, the number of CFU-Fs in peripheral blood of the DMOG group increased significantly (1.5 ± 0.58 vs. 2.5 ± 0.58, $P < 0.05$), and the number of CFU-Fs in bone marrow showed the same trend (9.3 ± 0.96 vs. 13.8 ± 0.96, $P < 0.01$) (Fig. 1a). The numbers of PB-MSCs and BM-MSCs were increased in rats treated with DMOG.

PB-MSC and BM-MSC Growth Curves, Cell Cycles and Migration Abilities are Similar We compared several biological characteristics between PB-MSCs and BM-MSCs. The latency period for the PB-MSCs was from day 1 to 3, and the logarithmic growth period was from day 4 to 6. The beginning of the plateau period for PB-MSCs was day 6. The latency period for BM-MSCs was from day 1 to 2, and the logarithmic growth period was from day 3 to 6. The beginning of the plateau period for BM-MSCs was day 6. The total number of BM-MSCs was significantly higher than that of PB-MSCs from day 3 to 7 ($P < 0.05$) (Fig. 1b). These results showed that BM-MSCs have stronger proliferation ability than PM-MSCs. In addition, PB-MSCs and BM-MSCs have similar latency, logarithmic growth and plateau phases, and their growth curves are S-shaped.

In G1 phase, PB-MSCs accounted for $71.59 \pm 4.70\%$, and BM-MSCs accounted for $58.55 \pm 0.99\%$. In G2 phase, PB-MSCs accounted for $18.59 \pm 2.58\%$, and BM-MSCs accounted for $26.60 \pm 0.47\%$. In S phase, PB-MSCs accounted for $10.25 \pm 0.64\%$, and BM-MSCs accounted for $14.00 \pm 0.47\%$. There were significantly fewer S phase PB-MSCs than BM-MSCs ($P < 0.05$) (Fig. 1c). These results indicated that the proliferation potential of PM-MSCs is weaker than that of BM-MSCs. In G1, G2 and S phases, the distribution of PB-MSCs and BM-MSCs was similar.

The migration of the SDF-1α cytokine to PB-MSCs and BM-MSCs was detected by a Transwell assay. PB-MSCs (108.6 ± 14.61) and BM-MSCs (133.4 ± 14.37) migrated to the lower transwell chamber by SDF-1α chemotaxis for 16 h. The number of migrated PB-MSCs was significantly lower than that of BM-MSCs ($P < 0.05$) (Fig. 1d). Thus, these data demonstrated that PB-MSCs have weaker migration ability in response to SDF-1α than BM-MSCs.

HIF-1 Pathway Increases in DMOG-Treated MSCs To explore the effect of DMOG on the HIF-1 pathway, we examined expression levels of HIF-1α, SDF-1α and VEGF using Western blotting and real-time qPCR. Compared to 0 μM DMOG, HIF-1α, SDF-1α and VEGF protein expression
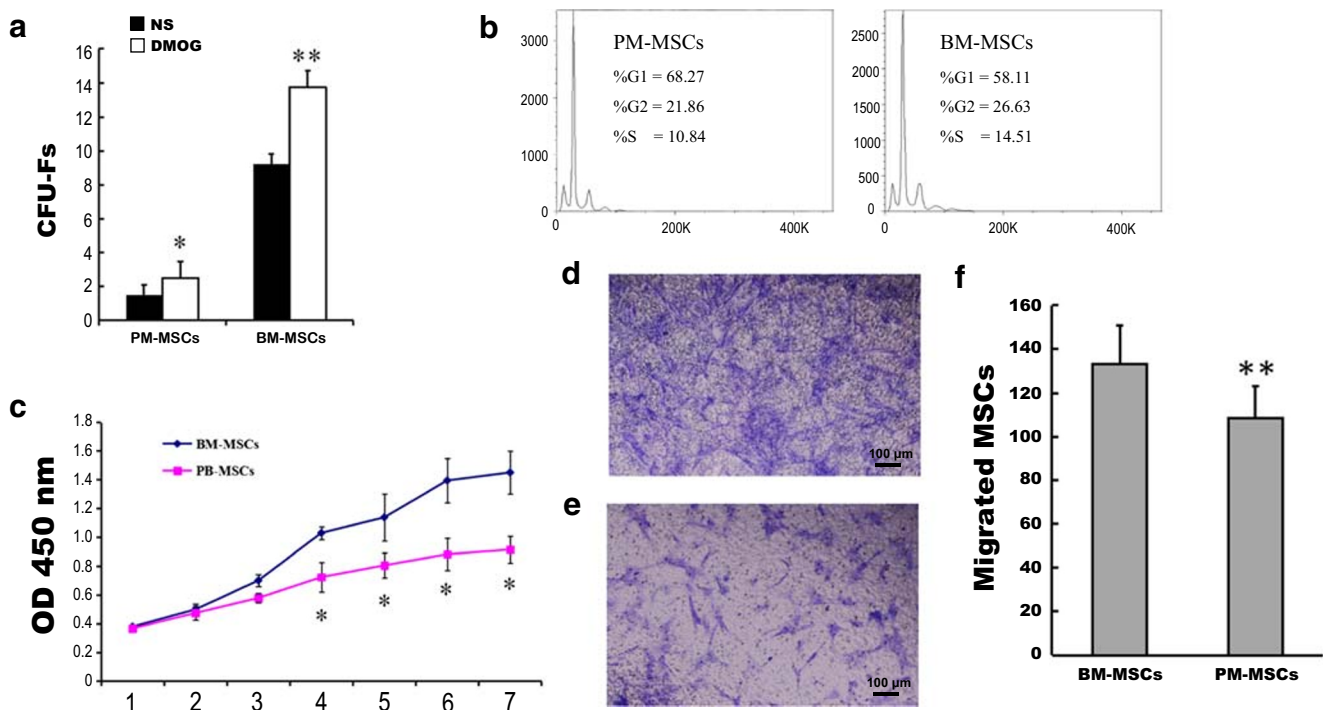
Fig. 1 MSCs in bone marrow are mobilized into peripheral blood by DMOG while maintaining similar abilities. **a** The numbers of MSCs in peripheral blood and bone marrow were detected by the CFU-F assay. **b** The growth curves of PB-MSCs and BM-MSCs were detected by CCK-8. **c** PB-MSC and BM-MSC cell cycles were detected by Flow cytometry. Transwell assay results and crystal violet staining of the BM-MSCs and PM-MSCs are shown in **d** and **e**, respectively. **f** The number of migrated MSCs. Scale bar = 100 μm. (*$P < 0.05$, **$P < 0.01$)

levels were significantly increased by 20 μM DMOG ($P < 0.01$). HIF-1α, SDF-1α and VEGF mRNA expression levels were significantly increased by treatment with 20 μM, 40 μM and 80 μM DMOG ($P < 0.01$). The highest expression levels of HIF-1α, SDF-1α and VEGF were found in the 20 μM DMOG group (Fig. 2). These results showed that the expression levels of HIF-1α, SDF-1α and VEGF in MSCs were significantly increased when treated with 20 μM DMOG. Thus, the expression levels of HIF-1 signaling pathway components may be regulated by 20 μM DMOG.

HIF-1α Knockdown Inhibits the HIF-1 Pathway in DMOG-Treated MSCs We first selected the appropriate HIF-1α siRNA concentration. For the utilized transfection method, 30 pM control siRNA showed the highest transfection rate ($P < 0.01$) for the siRNA positive control Block - IT ™ Alexa Fluor® Red Fluorescent oligo. Therefore, we selected 30 pM as the concentration for the HIF-1α siRNA ($P < 0.01$) (Fig. 3). In the HIF-1α siRNA group, the protein expression levels HIF-1α, SDF-1α and VEGF increased significantly in the 20 μM DMOG group compared to the 0 μM DMOG group ($P < 0.01$). At the same concentration, the expression levels of HIF-1α, SDF-1α and VEGF in the HIF-1α siRNA group were significantly reduced compared to the control siRNA group ($P < 0.01$) (Fig. 4).

In the control siRNA and HIF-1α siRNA groups, the mRNA expression levels of HIF-1α, SDF-1α and VEGF were significantly increased by 20 μM DMOG compared to 0 μM DMOG ($P < 0.01$). Moreover, the mRNA expression levels of HIF-1α, SDF-1α and VEGF in the HIF-1α siRNA group were significantly reduced compared to the control siRNA group ($P < 0.01$) (Fig. 4).

These results indicated that the HIF-1α, SDF-1α and VEGF levels were effectively reduced by the interference of HIF-1α and significantly upregulated by 20 μM DMOG.

Bone Marrow Microvessels are Increased in DMOG-Treated Rats To investigate the relationship among HIF-1α, SDF-1α and VEGF, we used immunohistochemical analysis to detect the number of bone marrow microvessels. The expression of VEGF was negative, as shown in Fig. 5a. The cytoplasm of bone marrow hematopoietic cells and vascular endothelial cells was yellow or brown, and the nucleus was blue, which indicated that the expression of VEGF was positive (Fig. 5b–f). Compared to the NS group, the number of microvessels in the DMOG group increased significantly ($25 \pm 2.57\%$ vs. $38.7 \pm 4.96\%$; $P < 0.05$). Compared to the DMOG group, the number of bone marrow microvessels in the SU5416 group was significantly decreased ($38.7 \pm 4.96\%$ vs. $24.7 \pm 2.06\%$; $P < 0.05$), and the number of the bone marrow microvessels was not significantly different between the YC-1 and AMD3100 groups ($38.7 \pm 4.96\%$ vs. $36.4 \pm 8.14\%$ and $38.7 \pm 4.96\%$ vs. $36.8 \pm 8.13\%$; $P > 0.05$) (Fig. 5g). The immunohistochemistry results revealed that DMOG increases the number of bone marrow microvessels in rats. Furthermore, the number of bone marrow microvessels decreased significantly after treatment with SU5416, which blocks the VEGF/VEGFR signaling pathway.
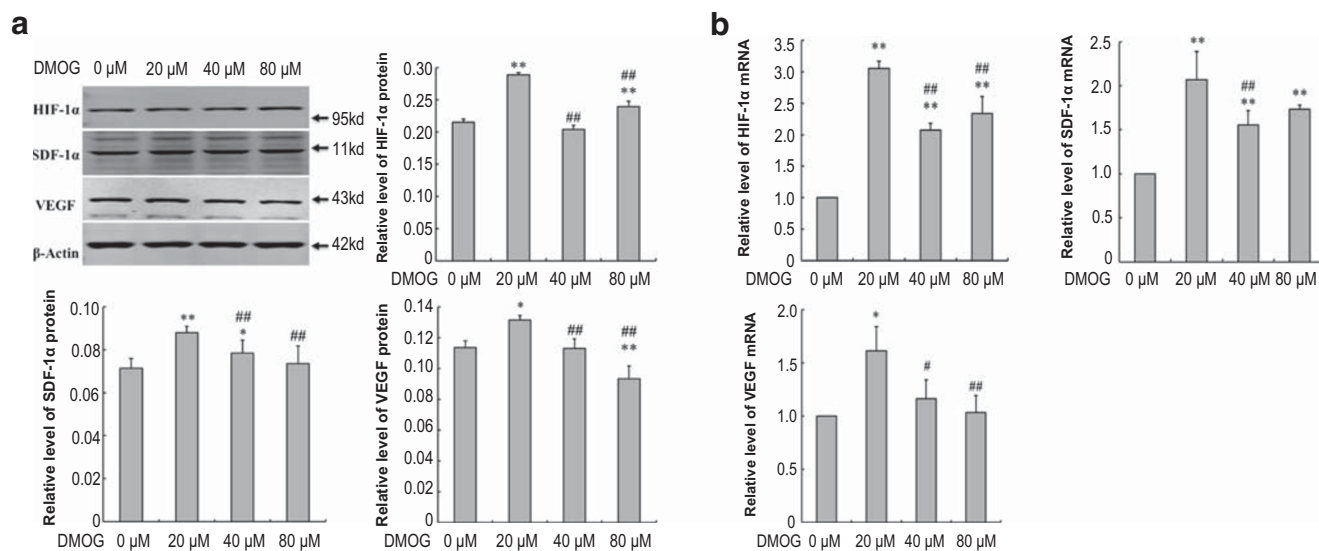
Fig. 2 HIF-1α, SDF-1α and VEGF expression levels in MSCs are increased by 20 μM DMOG. **a** The effect of DMOG on the protein levels of the HIF-1 signaling pathway components in MSCs. **b** The effect of DMOG on the mRNA levels of the HIF-1 signaling pathway components in MSCs. Significant difference compared to 0 μM DMOG (*$P < 0.05$, **$P < 0.01$). Significant difference compared to 20 μM DMOG (#$P < 0.05$, ##$P < 0.01$)
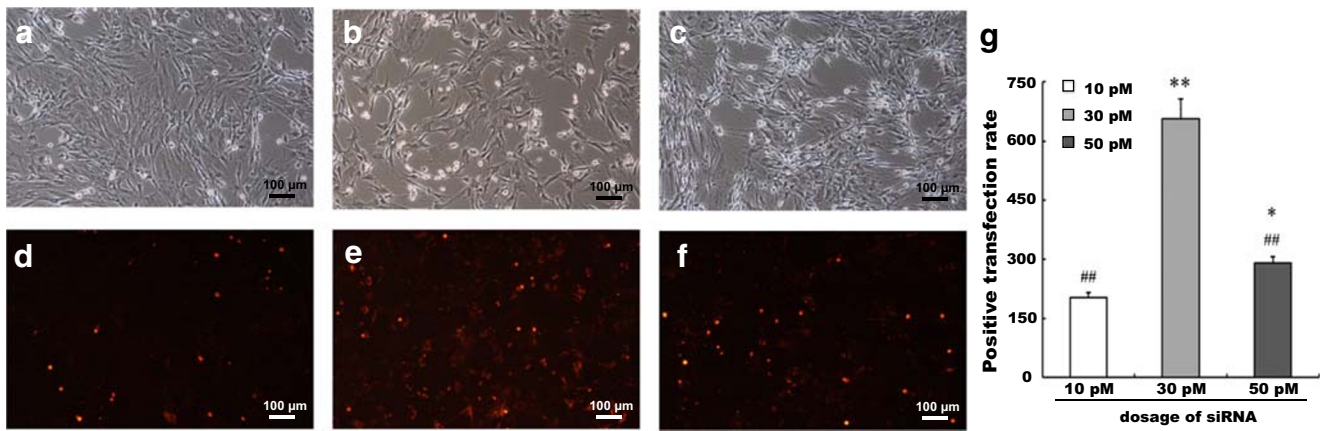
Fig. 3 HIF-1α siRNA dosage selection by transfection experiment. **a** and **b** Light source field and fluorescence light source field after transfection with 10 pM siRNA, **c** and **d** with 30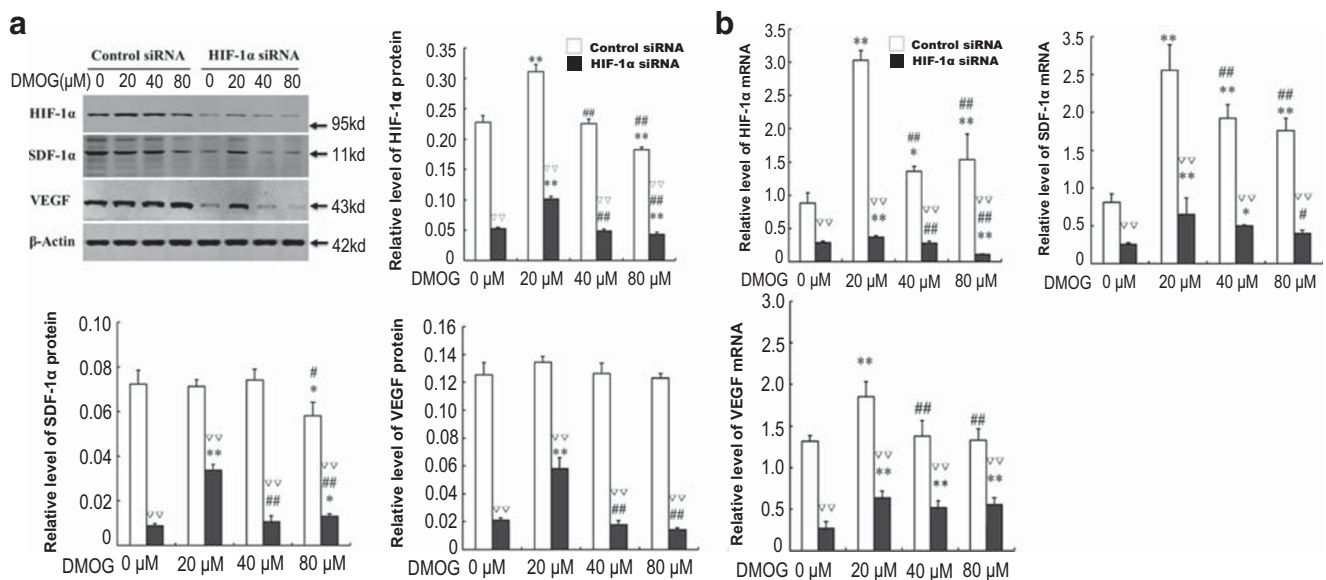pM siRNA, **e** and **f** with 50pM siRNA. Significant difference compared to 10 pM siRNA (*$P < 0.05$, **$P < 0.01$). Significant difference compared to 30 pM siRNA ($^{\#}P < 0.05$, $^{\#\#}P < 0.01$)

Discussion

The prolyl hydroxylase inhibitor, DMOG, has been increasingly studied with regard to stem cell therapy. In this study, we detected the number of MSCs in peripheral blood and bone marrow of rats treated with DMOG. The results verified that DMOG mobilizes MSCs to peripheral blood and that the cell growth, cell cycle and migration ability of PB-MSCs were similar to those of BM-MSCs. The reduction of telomerase activity and the expression of cell cycle regulatory proteins in PB-MSCs may be related to the weaker proliferation ability of PB-MSCs compared to BM-MSCs [29].

There may be several pathways that influence MSC mobilization, including the SDF1/CXCR4, SCF/cKit and PI3K/Akt signaling pathways [30–33]. We investigated the HIF-1α signaling pathway, and the results revealed that the siRNA-induced interference of HIF-1α gene expression was intensified by DMOG. We speculated that DMOG mobilizes MSCs by regulating the HIF-1α signaling pathway. Thus, the biological effects of DMOG occurred by acting on the HIF-1 signaling pathway.

In the present study, 20 μM DMOG significantly upregulated the protein expression of HIF-1α and SDF-1α in MSCs. Moreover, 20 μM, 40 μM and 80 μM DMOG increased the

Fig. 4 The HIF-1 pathway in DMOG-treated MSCs is inhibited by HIF-1α siRNA. **a** The effects of HIF-1α siRNA and DMOG on the HIF-1 signaling pathway proteins in MSCs. **b** The effects of HIF-1α siRNA and DMOG on the mRNA levels of the HIF-1 signaling pathway components in MSCs. Significant difference compared to 0 μM DMOG (*$P < 0.05$, **$P < 0.01$). Significant difference compared to 20 μM DMOG ($^{\#}P < 0.05$, $^{\#\#}P < 0.01$). Significant difference compared to the control siRNA group with the same concentration ($^{\triangledown\triangledown}P < 0.01$)
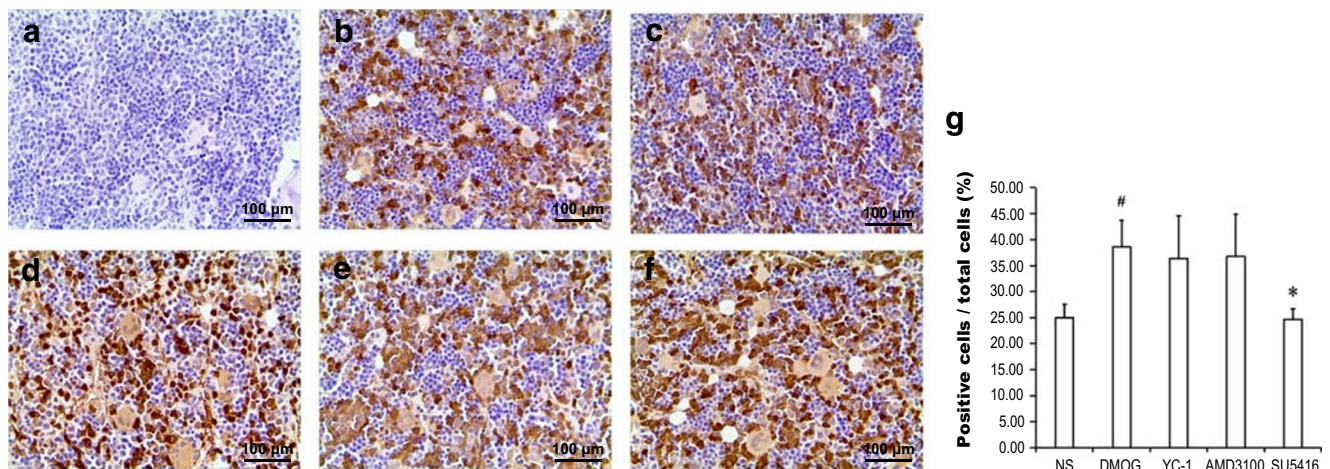
Fig. 5 DMOG increases bone marrow microvessels, but SU5416 blocks this increase. **a** Blank control group with immunohistochemical staining of bone marrow tissue. **b**, **c**, **d**, **e** and **f** Immunohistochemical staining for the NS, DMOG, YC-1, AMD3100 and SU5416 groups. Scale bar = 100 μm. Significant difference compared to the DMOG group (*$P < 0.05$). Significant difference compared to the SU5416 group (#$P < 0.05$)

mRNA expression of HIF-1α and SDF-1α in the control siRNA group. Among the DMOG treatments, 20 μM DMOG had the strongest effect. When HIF-1α was inhibited, the expression of SDF-1α was downregulated, and 20 μM DMOG effectively alleviated the effects of HIF-1α gene silencing, illustrating that DMOG plays an essential role not only in mobilizing MSCs but also in regulating HIF-1 and the downstream SDF-1 signaling pathway.

HIF-1α, a transcription factor, plays a major role in regulating VEGF [34–36]. VEGF promotes angiogenesis and anti-apoptotic effects. VEGF delays apoptosis and reduces the inflammatory response through hyperbaric oxygen therapy in a rat ischemia-reperfusion injury model [37]. The half-life of VEGF mRNA is extended after cells are transfected with HIF-1α [38]. Several studies have demonstrated that HIF-1α upregulates the VEGF receptor, thereby enhancing the biological effects of VEGF [39, 40]. Thus, we hypothesized that VEGF would be decreased after inhibiting HIF-1α in MSCs. In the present study, HIF-1α and VEGF expression levels were upregulated by 20 μM DMOG compared to 0 μM DMOG but downregulated in the HIF-1α siRNA group compared to the control group. After inhibition of HIF-1α, VEGF expression was downregulated, but 20 μM DMOG effectively alleviated the effects of HIF-1α interference. DMOG plays a vital role in mobilizing HIF-1 and its VEGF downstream signaling pathway in MSCs. Blockade of the VEGF/VEGFR signaling pathway by SU5416 reduced the number of bone marrow microvessels, thereby suggesting that the downstream VEGF/VEGFR signaling pathway directly regulated by HIF-1 plays an important role in DMOG-induced MSC mobilization.

In conclusion, DMOG mobilizes MSCs and upregulates the HIF-1 pathway. When HIF-1α is knocked down, the expression levels of its downstream molecules, namely, SDF-1α and VEGF, were decreased in MSCs. DMOG regulates the HIF-1α signaling pathway and promotes biological effects in MSCs. Upregulation of HIF-1 to directly regulate the SDF-1/CXCR4 and VEGF/VEGFR signaling pathways is crucial for MSCs. As a proline hydroxylase inhibitor, DMOG is a promising new agent for clinical applications as well as in the study of stem cell mobilization and bone injury; thus, the treatment of clinical diseases with DMOG has broad prospects.

Compliance with Ethical Standards

Conflict of Interest The authors declare no conflicts of interest.

References

1. Xu, K., Xiao, J., Zheng, K., Feng, X., Zhang, J., Song, D., et al. (2018). Mir-21/stat3 signal is involved in odontoblast differentiation of human dental pulp stem cells mediated by tnf-α. *Cellular Reprogramming, 20*(2), 107.

2. Lo, W. J., Lin, C. L., Chang, Y. C., Bai, L. Y., Lin, C. Y., Liang, J. A., et al. (2018). Total body irradiation tremendously impair the proliferation, differentiation and chromosomal integrity of bone marrow-derived mesenchymal stromal stem cells. *Annals of Hematology, 97*(4),697-707.

3. Gimble, J. M., Zvonic, S., Floyd, Z. E., Kassem, M., & Nuttall, M. E. (2006). Playing with bone and fat. *Journal of Cellular Biochemistry, 98*(2), 251.

4. Wu, L., Cai, X., Zhang, S., Karperien, M., & Lin, Y. (2013). Regeneration of articular cartilage by adipose tissue derived mesenchymal stem cells: Perspectives from stem cell biology and molecular medicine. *Journal of Cellular Physiology, 228*(5), 938–944.

5. Aubin, J.E. (2008). Chapter 4 - Osteoclast Biology: Regulation of Formation and Function. *Principles of Bone Biology,* 85-107.

6. Moroni, L., & Fornasari, P. M. (2013). Human mesenchymal stem cells: a bank perspective on the isolation, characterization and potential of alternative sources for the regeneration of musculoskeletal tissues. *Journal of Cellular Physiology, 228*(4), 680–687.

7. Yagi, H., Sotogutierrez, A., Parekkadan, B., Kitagawa, Y., Tompkins, R. G., Kobayashi, N., et al. (2010). Mesenchymal stem cells: mechanisms of immunomodulation and homing. *Cell Transplantation, 19*(6), 667–679.

8. Levesque, J.P., Winkler, I.G., Larsen, S.R., & Rasko, J.E. (2007). Mobilization of bone marrow-derived progenitors. *Handb Exp Pharmacol: Springer Berlin Heidelberg,* 3–36.

9. Link, D. (2010). Stem cells on the move. *Nature Medicine, 16*(10), 1073–1074.

10. Hoggatt, J., Speth, J. M., & Pelus, L. M. (2013). Concise review: sowing the seeds of a fruitful harvest: Hematopoietic stem cell mobilization. *Stem Cells, 31*(12), 2599.

11. Liu, W., Yu, Q., & Liu, L. (2013). Effect of prolylhydroxylase inhibitor on mobilization of mesenchymal stem cells in mice. *Journal of Zhejiang Chinese Medical University, 37*(12), 1371–1376.

12. Hu, S., Yu, Q., Liu, L., & Ge, T. (2015). Mechanism of hif-1 signaling pathway in mediating mscs mobilization with dmog. *Chinese Journal of Comparative Medicine, 25*(1), 9–14.

13. Liu, L., Yu, Q., Lin, J., Lai, X., Cao, W., Du, K., et al. (2011). Hypoxia-inducible factor-1α is essential for hypoxia-induced mesenchymal stem cell mobilization into the peripheral blood. *Stem Cells and Development, 20*(11), 1961–1971.

14. Hou, P., Kuo, C. Y., Cheng, C. T., Liou, J. P., Ann, D. K., & Chen, Q. (2014). Intermediary metabolite precursor dimethyl-2-ketoglutarate stabilizes hypoxia-inducible factor-1α by inhibiting prolyl-4-hydroxylase phd2. *PLoS One, 9*(11), e113865.

15. Voulgarelis, M., & Tsichlis, P. N. (2016). Proline hydroxylation linked to akt activation. *Science, 353*(6302), 870.

16. Cai, X., Yuan, Y., Liao, Z., Xing, K., Zhu, C., Xu, Y., et al. (2017). A-ketoglutarate prevents skeletal muscle protein degradation and muscle atrophy through phd3/adrb2 pathway. *FASEB Journal, 32*(1), 488.

17. Li, M., Sun, X., Ma, L., Jin, L., Zhang, W., Xiao, M., et al. (2017). SDF-1/CXCR4 axis induces human dental pulp stem cell migration through FAK/PI3K/Akt and GSK3β/β-catenin pathways. *Scientific Reports, 7*, 40161.

18. Arakura, M., Lee, S. Y., Takahara, S., et al. (2017). Altered expression of SDF-1 and CXCR4 during fracture healing in diabetes mellitus. *International Orthopaedics, 41*(6), 1211–1217.

19. Ghadge, S. K., Messner, M., Van, P. T., Doppelhammer, M., Petry, A., Görlach, A., et al. (2017). Prolyl-hydroxylase inhibition induces SDF-1 associated with increased cxcr4+/cd11b+ subpopulations and cardiac repair. *Journal of Molecular Medicine, 95*(8), 825–837.

20. Liu, H., Xue, W., Ge, G., Luo, X., Li, Y., Xiang, H., et al. (2010). Hypoxic preconditioning advances cxcr4 and cxcr7 expression by activating hif-1α in mscs. *Biochemical & Biophysical Research Communications, 401*(4), 509.

21. Niyaz, M., Gürpınar, Ö. A., Oktar, G. L., Günaydın, S., Onur, M. A., Özsin, K. K., et al. (2015). Effects of vegf and mscs on vascular regeneration in a trauma model in rats. *Wound Repair and Regeneration, 23*(2), 262.

22. Fong, G. H. (2019). Regulation of angiogenesis by oxygen sensing mechanisms. *Journal of Molecular Medicine, 87*(6), 549.

23. Pitchford, S. C., Furze, R. C., Jones, C. P., Wengner, A. M., & Rankin, S. M. (2009). Differential mobilization of subsets of progenitor cells from the bone marrow. *Cell Stem Cell, 4*(1), 62.

24. Shin, D. H., Kim, J. H., Jung, Y. J., et al. (2009). Preclinical evaluation of YC-1, a HIF inhibitor, for the prevention of tumor spreading. *Cancer Letters, 255*(1), 107–116.

25. Na, J. I., Na, J. Y., Choi, W. Y., et al. (2015). The HIF-1 inhibitor YC-1 decreases reactive astrocyte formation in a rodent ischemia model. *American Journal of Translational Research, 7*(4), 751–760.

26. Wang, X., Liu, C., Wu, L., et al. (2016). Potent ameliorating effect of hypoxia-inducible factor 1α (HIF-1α) antagonist YC-1 on combined allergic rhinitis and asthma syndrome (CARAS) in rats. *European Journal of Pharmacology, 788*, 343–350.

27. Li, J., & Oupický, D. (2014). Effect of biodegradability on CXCR4 antagonism, transfection efficacy and antimetastatic activity of polymeric Plerixafor. *Biomaterials., 35*(21), 5572–5579.

28. Kim, E. H., Lee, H., Jeong, Y. K., et al. (2016). Mechanisms of SU5416, an inhibitor of vascular endothelial growth factor receptor, as a radiosensitizer for colon cancer cells. *Oncology Reports, 36*(2), 763–770.

29. Lund, T. C., Tolar, J., & Orchard, P. J. (2008). Granulocyte colony-stimulating factor mobilized CFU-F can be found in the peripheral blood but have limited expansion potential. *Haematologica, 93*(6), 908–912.

30. Golan, K., Vagima, Y., Ludin, A., Itkin, T., & Lapidot, T. (2012). S1P promotes murine progenitor cell egress and mobilization via S1P1-mediated ROS signaling and SDF-1 release. *Blood, 119*(11), 2478–2488.

31. Hatzistergos, K. E., Saur, D., Seidler, B., Balkan, W., Breton, M., Valasaki, K., et al. (2016). Stimulatory effects of mscs on ckit+ cardiac stem cells are mediated by sdf1/cxcr4 and scf/ckit signaling pathways. *Circulation Research, 119*(8), 921. https://doi.org/10.1161/CIRCRESAHA.116.309281.

32. Chen, J., Crawford, R., Chen, C., & Xiao, Y. (2013). The key regulatory roles of the pi3k/akt signaling pathway in the functionalities of mesenchymal stem cells and applications in tissue regeneration. *Tissue Engineering. Part B, Reviews, 19*(6), 516–528.

33. Wang, G. D., Liu, Y. X., Wang, X., Zhang, Y. L., & Xue, F. (2017). The SDF-1/CXCR4 axis promotes recovery after spinal cord injury by mediating bone marrow-derived from mesenchymal stem cells. *Oncotarget, 8*(7), 11629–11640.

34. Harms, K. M., Lu, L., & Anna, C. L. (2010). Murine neural stem/progenitor cells protect neurons against ischemia by hif-1α–regulated vegf signaling. *PLoS One, 5*(3), e9767.

35. Chen, J., Lai, L., Liu, S., Zhou, C., Wu, C., Huang, M., et al. (2016). Targeting HIF-1α and VEGF by lentivirus-mediated RNA interference reduces liver tumor cells migration and invasion under hypoxic conditions. *Neoplasma, 63*(6), 934–940.

36. Zhou, F., Du, J., & Wang, J. (2017). Albendazole inhibits HIF-1α-dependent glycolysis and VEGF expression in non-small cell lung cancer cells. *Molecular and Cellular Biochemistry, 428*(1–2), 171–178.

37. Zhang, Q., Chang, Q., Cox, R. A., Gong, X., & Gould, L. J. (2008). Hyperbaric oxygen attenuates apoptosis and decreases inflammation in an ischemic wound model. *Journal of Investigative Dermatology, 128*(8), 2102.

38. Liu, L. X., Lu, H., Luo, Y., Date, T., Belanger, A. J., Vincent, K. A., et al. (2002). Stabilization of vascular endothelial growth factor mrna by hypoxia-inducible factor 1. *Biochemical & Biophysical Research Communications, 291*(4), 908–914.

39. Lee, J. C., Tae, H. J., Kim, I. H., Cho, J. H., Lee, T. K., Park, J. H., et al. (2016). Roles of HIF-1α, VEGF, and NF-κB in ischemic preconditioning-mediated neuroprotection of hippocampal CA1

pyramidal neurons against a subsequent transient cerebral ischemia. *Molecular Neurobiology, 54*(9), 6984–6998.

40. Gerber, H. P., Condorelli, F., Park, J., & Ferrara, N. (1997). Differential transcriptional regulation of the two vascular endothelial growth factor receptor genes flt-1, but not flk-1/kdr, is up- regulated by hypoxia[J]. *Journal of Biological Chemistry, 272*(38), 23659.

Publisher's Note Springer Nature remains neutral with regard to jurisdictional claims in published maps and institutional affiliations.